Contemporary Mathematics
https://ojs.wiserpub.com/index.php/CM/

Research Article

Mathematical Simulation for Influence of Thermocapillary Radiative MHD Unsteady Couple Stress Ternary Hybrid Nanofluid on Stretching Parallel Surface

Ali Rehman[1,2], Sudarmozhi K[2], Zeeshan Ali[3], Dragan Pamucar[4], Dolat khan[5], Abdullah Aziz Saad[1*]

[1] School of Mechanical Engineering, Universiti Sains Malaysia, Nibong Tebal, Penang, 14300, Malaysia
[2] Department of Mathematics, Saveetha School of Engineering, SIMATS, Chennai, Tamil Nadu, India
[3] Department of Information Management, National Yunlin University of Science and Technology, Douliu, Yunlin, Taiwan ROC
[4] Széchenyi István University, Győr, Hungary
[5] Faculty of Science, King Mongkut's University of Technology Thonburi (KMUTT), 126 Pracha Uthit Rd., Bang Mod, Thung Khru, Bangkok, 10140, Thailand
E-mail: azizsaad@usm.my

Received: 25 July 2025; **Revised:** 1 September 2025; **Accepted:** 5 September 2025

Abstract: This study aims to provide a thorough mathematical simulation of the effects of heat radiation and thermocapillarity on the time-dependent flow of couple stress ternary hybrid nanofluid across a stretching parallel surface in magneto-hydrodynamics. The ternary hybrid nanofluid consists of Ag, TiO_2, Al_2O_3 nanoparticles dispersed within a base fluid, blood, enhancing its thermal performance. The governing partial differential equations are converted into a system of nonlinear ordinary differential equations by applying the proper similarity transformations to model the flow's unstable behavior. After that, the Homotopy Analysis Method is used to solve these equations semi-analytically. The intricate interactions between radiative heat transport, thermocapillary forces induced by surface tension gradients, Lorentz force from the applied magnetic field, and couple stress effects are all captured in the simulation. The influence of main dimensionless parameters, including the magnetic parameter, couple stress parameter, nanoparticle volume fractions, dimensionless film thickness, unsteady parameter, thermal radiation parameter and Eckert number, on velocity profile, temperature profile, skin friction and Nusselt number in the form of graphs. According to the results, radiation improves the properties of heat transmission, whereas thermocapillarity dramatically changes the flow and thermal boundary layers. Furthermore, the fluid velocity is suppressed by the occurrence of magnetic fields and couple stress, providing information about possible control mechanisms in thermal management systems. The results' graphical and tabular representations demonstrate how sensitive the temperature and velocity fields are to the physical parameters at play. These findings offer significant new insights into thermal management technologies and energy systems that employ complex nanofluid compositions.

***Keywords*:** thermocapillarity impact, Ag, TiO_2, Al_2O_3, Homotopy Analysis Method, stretching surface

MSC: 76A10, 76A05, 76D05

DOI: https://doi.org/10.37256/cm.6620257996

1. Introduction

Three distinct kinds of nanoparticles dispersed in a base fluid make up a ternary hybrid nanofluid, an advanced sort of nanofluid. To get better thermal performance, the advantages of several nanoparticles, thermal, electrical, and chemical, are combined. Shear forces cause the fluid close to a stretching surface (flat plate, sheet, or curved surface) to flow when it moves and stretches in a particular direction (e.g., linearly or exponentially). The temperature and velocity gradients form in the boundary layer that is created as a result. The momentum and energy equation usually governs the flow of ternary hybrid nanofluids over stretched surfaces. Semi-numerical methods are used to solve this type of flow, which is frequently nonlinear and modelled using similarity transformations. Lone et al. [1] studied Magnetohydrodynamic (MHD) viscous fluid flow across a stretching sheet with changing characteristics, the Dufour and Soret diffusion phenomena. Hayat et al. [2] studied time-dependent MHD flow with slip conditions across an increasingly stretched sheet. Reddy et al. [3] studied the impression of chemical reactions on MHD natural convection flow past an exponentially covering sheet via a porous material with heat source/sink and viscous dissipation. Neethu et al. [4] studied MHD hybrid nanofluid flow across an exponential sheet with radiation and dissipation possessions using multiple linear regression. Li et al. [5] studied generalized Lie similarity revolutions for heat transport and unsteady flow when internal heating and thermal radiation are present. Mandal et al. [6] studied MHD micropolar fluid flow melting energy transfer over a stretched sheet with thermal radiation and slide. Nandhini et al. [7] studied the shared impact of the exponential and radiation absorption on a chemically reactive Casson fluid over a stretched sheet. Ragupathi et al. [8] studied three-dimensional convective Casson nanofluid flow across a stretching sheet with exponential heat source effects and Arrhenius activation energy. Sharma et al. [9] studied nanofluid flow over a sheet with an exponential energy source and the consequence of Arrhenius activation energy. Ahmad et al. [10] studied unsteady Maxwell nanofluid bioconvective flow in three dimensions across an expanding sheet with fluctuating chemical reactions and thermal conductivity. Alqahtani et al. [11] studied Casson hybrid nanofluid flow across a stretching sheet, where heat and mass are transferred. Mohana et al. [12] studied the properties of nanoparticle form on MHD Cu-water nanofluid flow on a sheet with energy source/sink and radiation. Souayeh et al. [13] studied ternary nanofluid flow numerically using gyrotactic microbes over an increasingly stretched sheet. Abbas et al. [14] studied the flow of a 2^{nd} grade micropolar nanofluid over an exponentially extending sheet using a permeable medium. Gopal et al. [15] studied nanofluid flow over a stretching sheet: a computational investigation of viscous dissipation with 1^{st} order chemical reactions and ohmic effects. Anwar et al. [16] computationally studied nanofluid flow in a nonlinear stretching sheet with induced magnetohydrodynamics. Li et al. [17] studied how stretching and buoyant forces affect heat transport in Burger fluid dynamics when thermal radiation and heat sources are important. Hayat et al. [18] studied Jeffrey fluid MHD stagnation-point flow on a stretched sheet heated by convection. Hussain et al. [19] studied Jeffrey nanofluid's radiative hydromagnetic flow via a stretched sheet. Ahmad et al. [20] studied mixed Jeffrey fluid flow with the magnetohydrodynamic effect past an exponentially extending sheet. Krishna et al. [21] studied radiation, chemical reaction, and slip effects on time-dependent Jeffreys nanofluid flow across a sheet. Habib et al. [22] studied carbon nanoparticle-containing MHD Jeffrey fluid flow past a stretching sheet with Newtonian heating effects and viscous dissipation. Turkyilmazoglu et al. [23] studied the suggestion of nonlinear similarity flows induced by stretching or moving sheets: electrospinning and atomisation with or without air resistance. Turkyilmazoglu et al. [24] studied the two models of innovative time-dependent solutions and unsteady heat and fluid flow caused by stretching or shrinking sheets. Turkyilmazoglu et al. [25] studied the movement of fluid between two parallel active surfaces. Loretz et al. [26] studied the Equations for the activation energy of crystallisation in modified chalcogenide glasses. Ding et al. [27] studied the magnetic-fluid-coated capillary long-period fibre gratings for magnetic field sensing. Eslamifar et al. [28] study the optical limitation and nonlinear responses of copper nanoparticles using the z-scan method. Rehman et al. [29] studied hybrid nanofluids with dynamic viscosity and viscous dissipation flow by mixed convection. Rehman et al. [30] studied heat transfer and analytical evaluation of CuO and MgO engine oil base nanofluid under the effect of convective boundary conditions, magnetic fields, and dynamic viscosity. Rehman et al. [31] studied the effects of viscous dissipation and magnetic fields on the thin-film unstable flow of GO-EG/GO-W nanofluids. Alshammari et al. [32] studied heat source/sink and oscillation amplitude conditions for Darcy nanofluid's periodic and time-mean fluctuating heat transfer along a nonlinear radiating plate. Majeed et al. [33] studied the significance of natural convection,

nanoparticle diameter, nanolayer, and sinusoidal wall temperature in water flow confronted to a vertical plate using finite element analysis. Benaissa et al. [34] studied power-law heat and mass transfer performance thermal radiation and joule heating characteristics of nanofluid flow. Alshammari et al. [35] study heat fluctuations and turbulent nanofluids with oscillatory radiation, gravity, and a Darcy-Forchheimer porous medium is analysed using finite differences using a vertical cone. Khedher et al. [36] studied the impact of changing density and thermal conductivity on the mass and heat transfer of MHD second-grade nanofluid along the surface of high-temperature polymers. When compared to single-nanoparticle nanofluids, ternary hybrid nanofluids that contain more than two types of nanoparticles offer improved thermal and flow characteristics. The convective heat and mass transfer behaviour that results from these fluids' interaction with a stretching surface is particularly important in a number of sophisticated industrial and technical operations. Important uses include. Molten polymers are stretched into sheets, fibres, or films during extrusion procedures. Because ternary hybrid nanofluids have better thermal conductivity, cooling the stretched surface with them guarantees more even and rapid cooling, improving the quality of the final product and its structural stability. Therefore, in the current research work, we investigated the mathematical simulation of the effects of heat radiation and thermocapillarity on the time-dependent flow of ternary hybrid nanofluid across a stretching parallel surface in Magnetohydrodynamics (MHD). Up to the authors information, this model is first-time study, semi-numerical, with a stress ternary hybrid nanofluid. The results of this particular system demonstrate several new applications in various industrial and engineering fields. The Homotopy Analysis Method (HAM) studies ternary hybrid nanoparticles in a non-Newtonian blood base using sophisticated Boundary Value Problem (Homotopy) (BVPh) 1.0 and BVPh 2.0 solvers. It yields high-accuracy solutions for the nonlinear system, exposing the intricate relationships and thermal effects in such fluids. The derived equations for solution transformations are analysed using the HAM technique, and the impacts of several elements on the non-dimensional temperature and velocity field of ternary hybrid nanofluids are discussed.

1.1 *Novelty of the work*

This study represents a pioneering mathematical simulation of the unsteady radiative Magnetohydrodynamic (MHD) flow of a couple stress ternary hybrid nanofluid over a stretching parallel surfaces with the combined effects of thermocapillarity, radiation, Marangoni convection, and complex nanoparticle interactions. The incorporation of three distinct nanoparticles (titania oxide, alumina oxide, and silver) suspended in a blood-base fluid, alongside a couple of stress and radiative phenomena, sets this work apart by merging advanced physical mechanisms rarely studied together. The use of semi-numerical approaches, like the Homotopy Analysis Method, to solve the nonlinear, coupled boundary-layer equations under such diverse multiphysics effects further advances the modeling of high-efficiency heat and momentum transfer in nanofluidic systems.

1.1.1 *Real-time applications*

The findings of this research have direct applicability in high-performance thermal management systems where enhanced heat transfer and precise flow control are crucial. Real-world applications include biomedical devices using blood-based nanofluids for hyperthermia or targeted drug delivery, highly efficient cooling systems in electronics and nuclear reactors, advanced energy storage systems, heat exchangers, and aircraft or space vehicle thermal protection where complex fluids are subjected to radiative and magnetic effects. The ability of ternary hybrid nanofluids to significantly boost thermal conductivity, stability, and temperature regulation makes them valuable in next-generation industrial and biomedical thermal applications.

1.1.2 *Research questions*

1. How does the combination of thermocapillarity, radiative effects, and MHD influence boundary-layer behavior in couple stress ternary hybrid nanofluids?

2. What are the impacts of nanoparticle volume fraction and type on the thermal and velocity boundary layers in blood-based ternary hybrid nanofluids?

3. How do the couple stress and viscous dissipation modify the heat transfer and flow profiles compared to classical nanofluids?

4. In what ways does the magnetic field alter temperature distribution and flow stability in stretching surfaces with ternary hybrid nanofluid flows?

5. How can the simulation framework guide the optimization of nanofluid properties for real-time biomedical and energy system applications?

2. Problem formation

Consider the 2D laminar unsteady and incompressible radiative flow of couple stress trihybrid nanofluid between two parallel surfaces with the consideration of the impact radiation and Marangoni convection. The flow is caused by the stretching surface with a stretching velocity $U_s = \frac{bx}{(1-at)}$, where a and b are both positive constants and h is the uniform thickness. The stretching sheet is subjected to a magnetic field $B = \frac{B_0}{\sqrt{(1-at)}}$. The nanoparticles Ag, TiO_2, Al_2O_3, mixed with base fluid blood. The main equations according to Noor et al. [37], for continuity, velocity and temperature filed.

Figure 1 shows the flow modelling geometry.

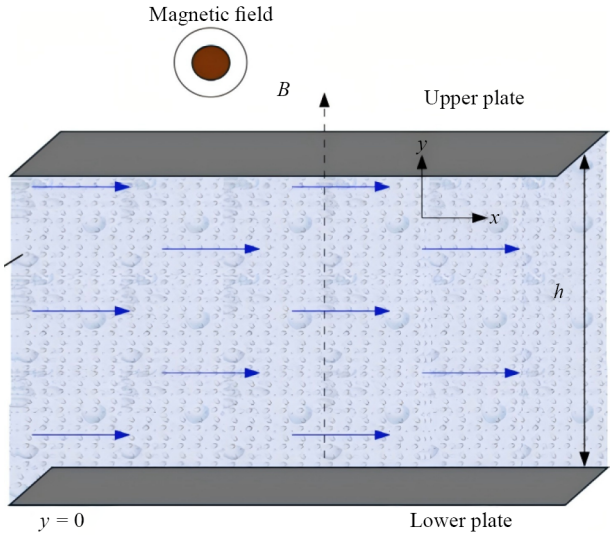

Figure 1. The flow modelling geometry

$$\frac{\partial u}{\partial x} + \frac{\partial v}{\partial y} = 0 \tag{1}$$

$$\frac{\partial u}{\partial t} + u\frac{\partial u}{\partial x} + v\frac{\partial u}{\partial y} = \nu_{\text{thnf}}\left(\frac{\partial^2 u}{\partial y^2}\right) - \frac{\sigma_{\text{thnf}}}{\rho_{\text{thn}}}B_0^2 u - \delta_0\frac{\partial^4 u}{\partial y^4}, \tag{2}$$

$$\frac{\partial T}{\partial t} + u\frac{\partial T}{\partial x} + v\frac{\partial T}{\partial y} = k_{\text{thnf}}\left(\frac{\partial^2 T}{\partial y^2}\right) + \frac{\mu_{\text{thnf}}}{(\rho C_p)_{\text{thnf}}}\left(\frac{\partial u}{\partial y}\right)^2 + \frac{16\sigma^* T_\infty^3}{3k^*}\frac{\partial^2 T}{\partial y^2} \tag{3}$$

Boundary conditions for mass, energy, and motion are created.

$$u = U_s,\ v = 0 =,\ T = T_s,\ \text{at } y = 0,$$
$$\mu \frac{\partial u}{\partial y} = \frac{\partial \sigma}{\partial x},\ \frac{\partial T}{\partial y} = 0,\ v = \frac{dh}{dt},\ \text{at } y = h, \tag{4}$$

Here u and v denote the velocity component in x and y, direction, t for time where T, is the temperature, the kinematic viscosity is ν, also σ represented the electric conductivity, ρ is the density and h is the uniform thickness. The surface tension exhibits a linear relationship with temperature.

$$\sigma = \sigma_0 \left(1 - \gamma (T - T_0)\right) \tag{5}$$

where γ is a fluid characteristic that is positive. Additionally, the velocity of the stretched surface is

$$U_s = \frac{bx}{(1 - at)} \tag{6}$$

Where a and b are both + ve constant.
Table 1 displays the thermophysical properties of titania oxide, alumina oxide silver and blood.

Table 1. The thermophysical properties of titania oxide, alumina oxide, silver, and blood

	$\rho\left(\frac{\text{kg}}{\text{m}^3}\right)$	$k\left(\frac{\text{W}}{\text{mK}}\right)$	$\sigma\left(\frac{\text{s}}{\text{m}}\right)$	$c_p\left(\frac{\text{j}}{\text{kgK}}\right)$	Pr
TiO_2	4,250	8.954	2.09×10^6	686.2	
Al_2O_3	3,970	40		765	
Ag	10,500	429		235	
Blood	4,250	0.492	0.60-0.80	3,594	20-40

Thermophysical properties for ternary hybrid nanofluid

$$\frac{\rho_{\text{thnf}}}{\rho_f} = \left(1 - \phi_{\text{TiO}_2}\right)\left[\left(1 - \phi_{\text{Ag}}\right)\left\{\left(1 - \phi_{\text{Al}_2\text{O}_3}\right) + \phi_{\text{Al}_2\text{O}_3}\frac{\rho_{\text{Al}_2\text{O}_3}}{\rho_f}\right\}\right] + \phi_{\text{TiO}_2}\frac{\rho_{\text{TiO}_3}}{\rho_f}, \tag{7}$$

$$\frac{\mu_{\text{thnf}}}{\mu_f} = \frac{1}{\left(1 - \phi_{\text{TiO}_2}\right)^{2.5}\left(1 - \phi_{\text{Ag}}\right)^{2.5}\left(1 - \phi_{\text{Al}_2\text{O}_3}\right)^{2.5}}, \tag{8}$$

$$\frac{k_{\text{thnf}}}{k_{\text{hnf}}} = \left\{\frac{k_{\text{TiO}_2} + 2k_{\text{hnf}} - 2\phi_{\text{TiO}_2}\left(k_{\text{hnf}} - k_{\text{TiO}_2}\right)}{k_{\text{TiO}_2} + 2k_{\text{hnf}} + \phi_{\text{TiO}_2}\left(k_{\text{hnf}} - k_{\text{TiO}_2}\right)}\right\}, \left\{\frac{k_{\text{Al}_2\text{O}_3} + 2k_{\text{hnf}} - 2\phi_{\text{Al}_2\text{O}_3}\left(k_{\text{hnf}} - k_{\text{Al}_2\text{O}_3}\right)}{k_{\text{Al}_2\text{O}_3} + 2k_{\text{hnf}} + \phi_{\text{Al}_2\text{O}_3}\left(k_{\text{hnf}} - k_{\text{Al}_2\text{O}_3}\right)}\right\},$$

$$\left\{\frac{k_{Ag}+2k_{\text{hnf}}-2\phi_{\text{Ag}}\left(k_{\text{hnf}}-k_{Ag}\right)}{k_{Ag}+2k_{\text{hnf}}+\phi_{\text{Ag}}\left(k_{\text{hnf}}-k_{Ag}\right)}\right\}, \tag{9}$$

$$\frac{(\rho C_p)_{\text{thnf}}}{(\rho C_p)_f}=\left(1-\phi_{\text{TiO}_2}\right)\left[\left(1-\phi_{\text{Ag}}\right)\left\{\left(1-\phi_{\text{Al}_2\text{O}_3}\right)+\phi_{\text{Al}_2\text{O}_3}\frac{(\rho C_p)_{\text{Al}_2\text{O}_3}}{(\rho C_p)_f}\right\}\right]+\phi_{\text{TiO}_2}\frac{(\rho C_p)_{\text{TiO}_3}}{(\rho C_p)_f}, \tag{10}$$

$$\frac{\sigma_{\text{thnf}}}{\sigma_{\text{hnf}}}=\frac{(1+2\phi_{\text{Ag}})\sigma_{Ag}+\left(1-2\phi_{\text{Ag}}\right)\sigma_{\text{hnf}}}{\left(1-\phi_{\text{Ag}}\right)\sigma_{Ag}+\left(1+\phi_{\text{Ag}}\right)\sigma_{\text{hnf}}},\ \frac{\left(1+2\phi_{\text{Al}_2\text{O}_3}\right)\sigma_{\text{Al}_2\text{O}_3}+\left(1-2\phi_{\text{Al}_2\text{O}_3}\right)\sigma_{nf}}{\left(1-\phi_{\text{Al}_2\text{O}_3}\right)\sigma_{Al_2O_3}+\left(1+\phi_{\text{Al}_2\text{O}_3}\right)\sigma_{nf}},$$

$$\frac{\left(1+2\phi_{\text{TiO}_2}\right)\sigma_{\text{TiO}_2}+\left(1-2\phi_{\text{TiO}_2}\right)\sigma_f}{\left(1-\phi_{\text{TiO}_2}\right)\sigma_{\text{TiO}_2}+\left(1+\phi_{\text{TiO}_2}\right)\sigma_f}. \tag{11}$$

Along with the Boundary Conditions (BCs) (4), the authors apply the similarity revolution to convert the Partial Differential Equation (PDEs) (1)-(3) into Ordinary Differential Equation (ODEs). The following formulas provide a clear definition of how to express these components in non-dimensional form.

$$\eta=\sqrt{\frac{b}{v}}\frac{y}{\sqrt{(1-at)}\beta},\ u=\frac{bx}{\sqrt{(1-at)}}f'(\eta),\ v=-\frac{\sqrt{vb}}{\sqrt{(1-at)}}\beta f(\eta),$$

$$T=T_0-T_{\text{ref}}\frac{bx^2}{2v}(1-at)^{-\frac{3}{2}}\theta(\eta), \tag{12}$$

$$\frac{\mu_{\text{thnf}}}{\mu_f}\frac{\rho_f}{\rho_{\text{thnf}}}f'''-\gamma\left(ff''-\frac{S}{2}\eta f''-\left(f'\right)^2-(S+Ma)f'\right)-\delta\frac{\mu_{\text{thnf}}}{\mu_f}\frac{\rho_f}{\rho_{\text{thnf}}}f^{iv}=0, \tag{13}$$

$$\frac{k_{\text{thnf}}}{k_f}\left(1+\frac{4}{3}R\right)\left(\theta''\right)+\gamma\left(f\theta'-2\theta f'-\frac{S}{2}\eta\theta'-\frac{3}{2}S\theta\right)+\frac{(\rho C_p)_{\text{thnf}}}{(\rho C_p)_f}Ec\left(f''\right)^2=0. \tag{14}$$

Boundary conditions are

$$\begin{aligned}&f(\eta)=0,\ f'(\eta)=1,\ \theta(\eta)=1,\ \text{ at } \eta=0,\\ &f(\eta)=\frac{1}{2}S,\ f''(\eta)=M\theta(\eta),\ \theta'(\eta)=0,\ \text{ at } \eta=1.\end{aligned} \tag{15}$$

Where $R=\frac{16\sigma^*T_\infty^3}{3k_fk^*}$, is the radiation parameter, $\beta=\sqrt{\frac{b}{v}}\frac{1}{\sqrt{(1-at)}}h(t)$ is the dimensionless film thickness, $\delta=\frac{\delta_0}{v^2{}_{bf}\rho_{bf}}$, shows couple stress parameter, $Ma=\frac{\sigma_fB_0^2}{\rho_fb}$, is the Hartmann number, the Eckert number is defined as $Ec=\frac{(U_s)^2}{C_p\left(T_0-T_s\right)}$ the dimensionless unsteadiness, parameter is $S=\frac{b}{a}$, the prandtl number is $\text{Pr}=\frac{\mu_fc_p}{k_f}$ and the thermocapillarity number is $M=\frac{\sigma_0T_{\text{ref}}\beta}{\mu\sqrt{bv}}$.

The Nu and C_f are key physical parameters in this study, defined as follows

$$C_{fx} = \frac{2\tau_w}{U^2\rho_f},\ Nu_x = \frac{xq_w}{k_{\text{thnf}}T_{\text{ref}}} \tag{16}$$

The non-dimension form of equation (16) is as

$$\text{Re}_x C_{fx} = \frac{2}{\beta}\left(f''(0)\right),\ Nu_x = \frac{1}{2\beta\sqrt{(1-at)}}\frac{k_{\text{thnf}}}{k_f}\left(\theta'(0)\right)\text{Re}_x^{\frac{3}{2}} \tag{17}$$

3. Methodology

The study formulates the two-dimensional, unsteady, incompressible radiative flow of a couple stress ternary hybrid nanofluid between two parallel stretching surfaces, incorporating the effects of thermocapillarity and Marangoni convection. The governing equations for mass, momentum, and energy are derived considering MHD, viscous dissipation, and radiative heat transfer, then non-dimensionalized using similarity transformations. The system's highly nonlinear ordinary differential equation set is solved using the Homotopy Analysis Method (HAM) to analyze the influence of key parameters such as the Eckert number, nanoparticles' volume fraction, and couple stress on the temperature and velocity fields within the boundary layer. Science and engineering frequently deal with nonlinear problems, which can be successfully resolved with the series solution. The HAM is an extremely efficient and modern approach to solving coupled nonlinear equations. The most recent HAM-based software tools, BVPh 1.0 and BVPh 2.0, aim to improve mathematical model convergence. The one with the fastest convergence is BVPh 2.0. The following approach yields the first solution.

$$F_0(\eta) = \frac{1}{2}e^{-2\eta},\ \theta_0(\eta) = e^{-\eta} \tag{18}$$

The linear operator in the aforementioned investigation is provided as

$$L_{f_1}(f_1) = f_1^{iv} - f_1''',\ L_\theta(\theta) = \theta'' \tag{19}$$

They have the following form.

$$L_{f_1}\left(D_1 + D_2\eta + D_3\eta^2\right) = 0,\ \text{ and } L_\theta\left(D_7 + D_8\eta\right) \tag{20}$$

For the consider problem the initial solution is given below.

$$f_0(\eta) = 1 - e^{-\eta},\ \theta(\eta) = e^{-\eta} \tag{21}$$

Here are the complete solutions of the nonlinear operators N_θ and N_{f_1}, which contain the constants,

$$\frac{d^3 f_1(\eta,\, r_1)}{d\eta^3} - \gamma\left((f_1(\eta,\, r_1))\frac{d^2 f_1(\eta,\, r_1)}{d\eta^2} - \frac{S}{2}\eta\frac{d^2 f_1(\eta,\, r_1)}{d\eta^2}\left(\frac{d f_1(\eta,\, r_1)}{d\eta}\right)^2\right)$$

$$+\gamma(S+Ma)\frac{d f_1(\eta,\, r_1)}{d\eta} - \delta\frac{d^5 f_1(\eta,\, r_1)}{d\eta^5} = 0 \tag{22}$$

$$\left(\left(1+\frac{4}{3}R\right)\frac{d^2\theta(\eta,\, r_1)}{d\eta^2}\right) + \gamma\left(f_1(\eta,\, r_1)\frac{d\theta(\eta,\, r_1)}{d\eta} - 2\frac{d f_1(\eta,\, r_1)}{d\eta}\theta(\eta,\, r_1)\right)$$

$$-\gamma\left(\frac{S}{2}\eta\frac{d\theta(\eta,\, r_1)}{d\eta} + \frac{3}{2}S\theta(\eta,\, r_1)\right) + \Pr Ec\left(\frac{d^2 f(\eta,\, r_1)}{d\eta^2}\right)^2 = 0. \tag{23}$$

According to [38–45], the basic concept of HAM for Eqs. (22)-(23) is as follows:

$$L_\theta\left[\theta(\eta,\, r_1) - \theta_0(r_1)\right]\left[1 - r_1\right] = N_\theta r_1 h_\theta\left[\theta(\eta,\, r_1)\right], \tag{24}$$

$$\left[1 - r_1\right] L_{f_1}\left[f_1(\eta,\, r_1) - f_0(r_1)\right] = r_1 h_{f_1} N_{f_1}\left[f_0(\eta,\, r_1)\right]. \tag{25}$$

When $r_1 = 0$ and $r_1 = 1$ the main section stated as

$$F(\eta,\, 1) = F(\eta) \text{ and } \theta(\eta,\, 1) = \theta(\eta), \tag{26}$$

such that $r_1 \in [0,\, 1]$, is we take: about $r_1 = 0$ of $\theta(\eta,\, r_1)$ and $f_1(\eta,\, r_1)$, the expansion of Taylor's series, are

$$f_1(\eta,\, r_1) = f_0(\eta) + \sum_{e=0}^{\infty} f_e(\eta) r_1^e, \tag{27}$$

$$\theta(\eta,\, r_1) = \theta_0(\eta) + \sum_{e=0}^{\infty} \theta_e(\eta) r_1^e. \tag{28}$$

4. Discussion

The computational results for the temperature field, velocity field, skin friction, and Nusselt number for two-dimensional radiation and thermocapillarity on the time-dependent flow of couple stress ternary hybrid nanofluid across a stretching parallel surface in Magnetohydrodynamics (MHD) are presented in this subsection. For a number of parameters, including unsteady parameter, magnetic parameter, nanoparticle volume fraction, radiation parameter, couple stress parameter, dimensionless film thickness, thermocapillarity number and Ec on the Nusselt number, skin friction, temperature and velocity and velocity field of ternary hybrid nanofluids. For this reason, Figures 2-10 have been created. Table 1 lists the thermophysical features of the base fluid, blood and nanoparticles. The resulting error is plotted in contradiction to the number of iterations in Table 2. The comparison of the current work with Sandeep et al. [46] is

presented in Table 3. Comparative changes in the skin friction coefficient and Nusselt number for various ternary hybrid nanofluid flow controlling parameters are shown in Table 3. The findings demonstrate how variations these parameters have distinct effects on skin friction and Nusselt number. Furthermore the values of skin friction and Nusselt number obtained by the thesis have close agreement with the work published by Sandeep et al. [46] publish work.

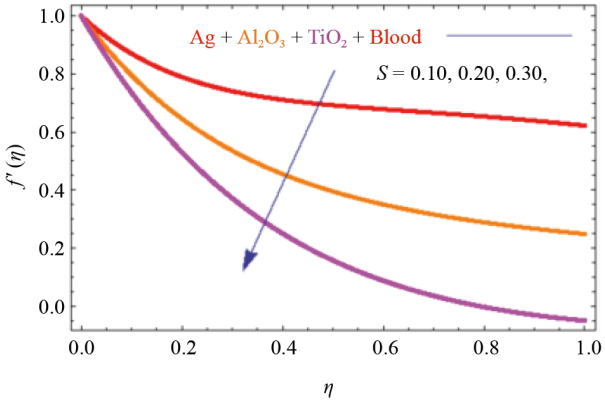

Figure 2. Impact of unsteady parameter via velocity filed

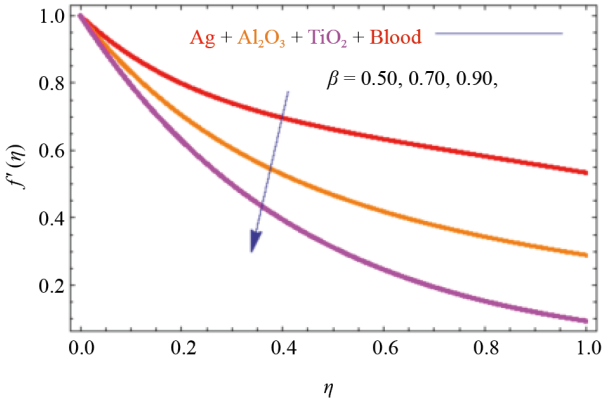

Figure 3. Impact of dimensionless film thickness via velocity filed

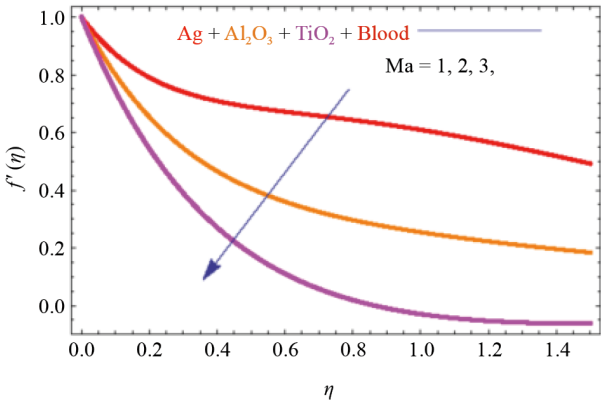

Figure 4. Impact of MHD parameter via velocity filed

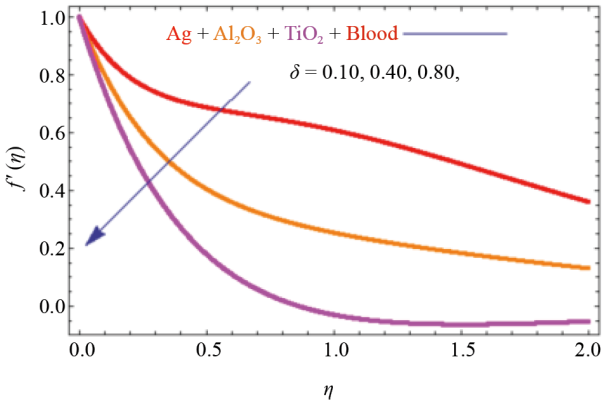

Figure 5. Impact of couple stress parameter via velocity filed

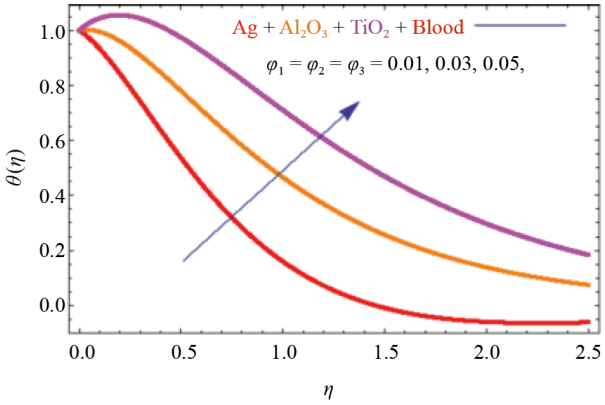

Figure 6. Influence of nanoparticles volume friction via temperature

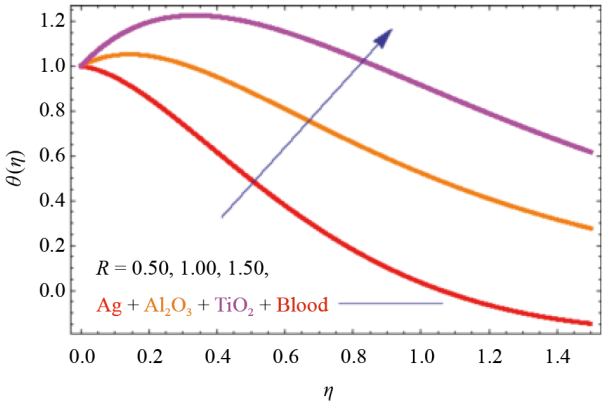

Figure 7. Impact of radiation parameter via temperature filed

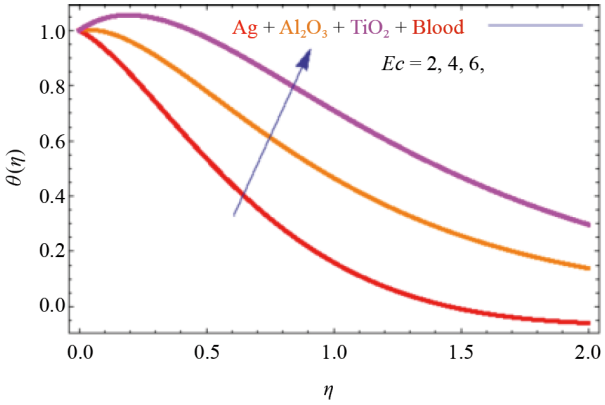

Figure 8. Influence of Eckert number via temperature filed

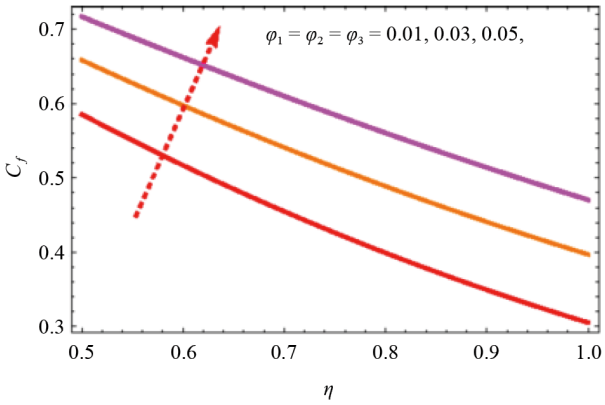

Figure 9. Impact of nanoparticles volume friction via skin friction

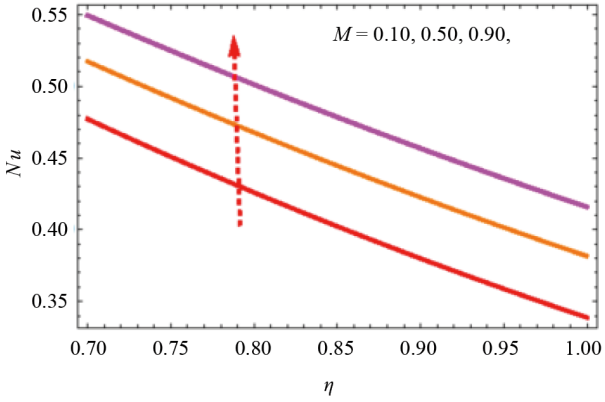

Figure 10. Impact of thermocapillarity number via Nusselt number

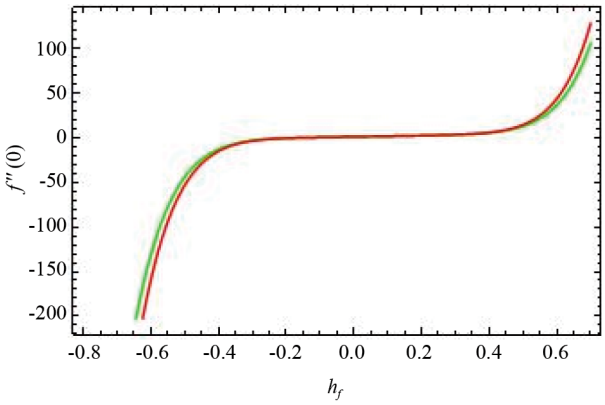

Figure 11. Convergence control parameter for HAM

Table 2. Explains how the $f'(\eta)$ and $\theta(\eta)$ converge

n	Velocity equation	Temperature equation
1	1.5171×10^{-1}	1.3924×10^{-1}
5	1.6945×10^{-2}	1.4536×10^{-2}
10	1.8551×10^{-3}	1.5645×10^{-3}
15	1.9564×10^{-4}	1.6756×10^{-4}
20	1.2395×10^{-5}	1.8463×10^{-5}

Table 3. shows the comperision of current work with Sandeep et al. [46]

C_f [46] result	C_f Present results	Nu [46] result	Nu Present results
-1.5417	-1.3651	2.3023	1.9963
-1.817	-1.7291	1.8432	2.0063
-2.0565	-1.8365	1.5673	1.1163
-1.5417	-1.1062	2.3023	2.1634
-1.5417	-1.2766	1.5776	2.0158
-1.5417	-1.2106	1.1852	1.7326
-1.5417	-1.2706	2.3023	3.1440
-1.3459	-1.3048	2.5471	3.6040
-1.2459	-1.1932	2.7366	1.8341
-1.5417	-1.4106	2.3023	3.2963
-1.6281	-1.5306	2.1355	3.1062
-1.7321	-1.6306	1.9643	1.1362
-1.1078	-1.0146	0.1274	1.2463
-1.5417	-1.2077	2.3023	2.2963
-1.8972	-1.7148	4.2884	4.8430
-1.5417	-1.3206	2.3023	2.1573
-1.7264	-1.6988	3.3141	3.8976
-1.8972	-1.8311	4.2884	4.6378
-1.6489	-1.4930	1.7294	0.9640
-1.5882	-1.4718	1.9443	1.2460
-1.5417	-1.3306	2.3023	2.0976

A type of nanofluid, defined as ternary hybrid nanofluids, or Ternary Hybrid Nanofluids (THNFs), is made up of three different types of nanoparticles distributed throughout a base fluid. These particles may be metallic, ceramic, or polymeric. When combined, these nanoparticles increase the base fluid's thermal conductivity, stability, and efficiency of heat transmission. All things considered, ternary hybrid nanofluids could be used in a variety of industries, including energy production, electronics cooling, and medical therapies. Researchers have attempted to investigate the mechanics of heat transmission in order to evaluate the structure of nanofluids and determine their potential for heat transfer. The heat transmission capacity of ternary hybrid nanofluids is significantly larger than that of binary and hybrid nanofluids.

The outcome of the unsteady parameter on the velocity field of ternary hybrid nanofluids is depicted in Figure 2. The velocity field decreases as the unsteady parameter rises. The velocity field of ternary hybrid nanofluids is significantly inclined by the unstable parameter, which is frequently represented by symbols like. The time-dependent character of the flow is represented by the unsteady parameter. Generally speaking, a more transitory or quickly changing flow field is indicated by a greater value of this parameter. When fluid flow is not steady-state, that is, when velocity and other variables change over time, it physically appears in governing equations. The velocity field tends to decrease as the unstable parameter rises. This occurs as a result of flow retardation, which occurs when the system requires time to adapt to abrupt changes. Unsteadiness causes inertia, which resists acceleration and lowers the magnitude of velocity. In velocity profiles, the velocity curve's peak usually shifts closer to the surface when the unstable parameter is improved.

The effect of dimensionless film thickness on the velocity field of ternary hybrid nanofluids is depicted in Figure 3. The velocity field declines as the dimensionless film thickness increases. The behaviour of Ternary Hybrid Nanofluid (THNF) flow is significantly prejudiced by the dimensionless film thickness parameter, particularly in thin film or boundary layer difficulties. The relative thickness of the fluid layer (or film) across a stretching or moving surface is described by the dimensionless film thickness. Typically, it is described as the physical film thickness divided by a particular length scale, like the width of the border layer or the stretching length. The velocity field of the ternary hybrid nanofluid typically decreases as the dimensionless film thickness parameter rises. This is because the flow domain expands, diluting the momentum caused by stretching and lowering the velocity gradient.

The outcome of the MHD parameter on the velocity field of ternary hybrid nanofluids is depicted in Figure 4. The velocity field declines as the M increases. The outcome of a magnetic field on an electrically conducting fluid is represented by the MHD parameter. Because of their increased electrical conductivity, Ternary Hybrid Nanofluids (THNFs), which comprise a suspension of 3 different kinds of nanoparticles in a base fluid, are especially affected by MHD. A resistive force is introduced by the Lorentz force, which faces the fluid flow. As a result, the fluid velocity across the boundary layer decreases. The velocity field of ternary hybrid nanofluids significantly decreases as the MHD value increases. The magnetic field's Lorentz force, which functions as a resistive drag against fluid velocity, is responsible for this.

The outcome of the couple stress parameter on the velocity field of ternary hybrid nanofluids is depicted in Figure 5. The velocity field declines as the couple stress parameter rises. In fluid models that take into consideration microstructural effects in non-Newtonian fluids, such as couple stress fluids, the couple stress parameter is employed. Couple stress effects enable more precise modelling of flow characteristics in microfluidic or non-continuum regimes in the setting of Ternary Hybrid Nanofluids (THNFs), which comprise a complicated suspension of three distinct nanoparticles. The micropolar or couple stress fluid theory, which takes into account body couplings and fluid rotational interactions, is where the couple stress parameter originates. The velocity field of ternary hybrid nanofluids declines as the coupling stress parameter rises. This is because fluid particles' linear mobility is impeded by microstructural interactions and increased rotational resistance.

The outcome of the nanoparticles volume friction on the temperature field of ternary hybrid nanofluids is depicted in Figure 6. The temperature field increases as the volume friction increases. The percentage of solid nanoparticles suspended in a base fluid is represented by the nanoparticles' volume fraction. This parameter has a significant effect on the thermal behaviour of Ternary Hybrid Nanofluids (THNFs), which are composed of three distinct kinds of nanoparticles. The nanofluid's effective thermal conductivity and energy capacity are directly impacted by the volume fraction. Greatly improves thermal conductivity, which improves heat distribution and absorption. Better thermal diffusion across the fluid layer is indicated by the thickening of the temperature boundary layer. The energy field of ternary hybrid nanofluids is

significantly improved by a rise in the volume fraction of nanoparticles. This is because the nanofluid's enhanced thermal conductivity and energy transport properties lead to thicker energy boundary layers and higher temperature dispersion.

The effect of R on the temperature field of ternary hybrid nanofluids is depicted in Figure 7. The temperature field increases as the R increases. The impact of R on fluid energy transfer is measured by the radiation parameter. In high-temperature applications like solar collectors, nuclear cooling, or aerospace thermal systems, radiative heat transfer plays a crucial role in Ternary Hybrid Nanofluids (THNFs), which are composed of 3 different kinds of nanoparticles suspended in a base fluid. Increases the fluid's total heat content, which raises the temperature field. Deeper heat penetration into the fluid domain is indicated by a thicker thermal boundary layer. The temperature field of ternary hybrid nanofluids rises as the R increases. This is brought about by improved radiative heat transfer, which raises the fluid's internal thermal energy and creates thicker thermal boundary layers.

The outcome of Ec on the temperature field of ternary hybrid nanofluids is depicted in Figure 8. The temperature field rises as the Ec increases. The ratio of kinetic energy to thermal energy in a fluid flow is represented by the dimensionless Ec. The Ec is essential for viscous dissipation and temperature raising in high-speed or high-shear flows in Ternary Hybrid Nanofluids (THNFs), which blend three distinct nanoparticle types to improve thermal performance leading to increased viscous dissipation, which is the conversion of mechanical energy into thermal energy, raising the temperature of the fluid, particularly in areas with large velocity gradients. The temperature field of ternary hybrid nanofluids increases as the Eckert number rises. This is because of increased viscous dissipation effects, which thicken the thermal boundary layer and raise fluid temperature by converting kinetic energy into heat.

The outcome of the nanoparticles volume friction on the skin friction of ternary hybrid nanofluids is depicted in Figure 9. The skin friction increases as the volume friction increases. Skin friction, which is the tangential shear stress acting on the surface as a result of fluid viscosity, is greatly influenced by the volume fraction of nanoparticles in Ternary Hybrid Nanofluids (THNFs). Changes in the fluid's rheological characteristics, such as its density and viscosity, impact the skin friction coefficient in THNFs, which are composed of three different kinds of nanoparticles. The skin friction of ternary hybrid nanofluids increases as the volume percentage of nanoparticles increases. Increased viscosity and momentum diffusion cause this, which raises surface drag and shear stress at the wall.

The effect of thermocapillarity number on the Nusselt number of ternary hybrid nanofluids is depicted in Figure 10. The Nusselt number rises as the thermocapillarity number rises. The impact of temperature-dependent surface tension, commonly referred to as the Marangoni effect, on fluid flow is slowed by the thermocapillarity number. Thermocapillarity is essential for surface-driven convection in Ternary Hybrid Nanofluids (THNFs), which mix three different kinds of nanoparticles to improve thermal performance, particularly in thin films or microfluidic applications, strengthens surface-driven convection by increasing surface tension gradients. This enhances thermal transfer close to the surface because the thermocapillary flow more efficiently removes thermal energy from the heated surface. The Nusselt number of ternary hybrid nanofluids rises in proportion to the thermocapillarity number. Stronger thermally generated surface tension gradients, which amplify Marangoni convection and encourage improved surface cooling, are the cause of this increase in convective heat transfer. Figure 11 shows the h curve for HAM solution, which shows the rate of convergence.

5. Conclusion

This research paper investigates the mathematical simulation of the effects of heat radiation and thermocapillarity on the time-dependent flow of magnetohydrodynamic couple stress ternary hybrid nanofluid across a stretching parallel surface with the impact of viscous dispersion, radiation and Marangoni convection. The trihybrid nanofluid made of Ag, TiO_2, Al_2O_3, nanoparticles with base fluid blood. The temperature equation takes into account the outcome of radiation and viscous dissipation. The leading transport equations are transformed into a system of initial value problems by applying suitable similarity transformations. The main conclusions are highlighted by data tabulation and graphical displays.

a. Velocity field of ternary hybrid nanofluid is inversely related, magnetohydrodynamic parameter, unsteady parameter, dimensionless film thickness and couple stress parameter.

b. The temperature field is increasing as the radiation parameter, nanoparticles volume friction and Eckert number rise.

c. Skin friction increases with the nanoparticles' volume friction.

d. The Nusselt number increases as the thermocapillarity number increases.

e. The residual error decreases as the number of iterations rises.

6. Limitations

Several limitations exist in this study. The mathematical model assumes laminar, two-dimensional, and incompressible flow, which may not fully capture complex 3D or turbulent behaviors found in industrial setups. Nanoparticle aggregation, possible slip between phases, and chemical reactions are neglected for simplicity. While the HAM provides semi-analytical solutions, experimental validation is absent, and the bio-compatibility or long-term stability of the ternary hybrid nanofluid (especially with blood as a base fluid) is not addressed. Finally, the considered geometry and boundary conditions may not cover all practical engineering scenarios.

7. Future work

Building on this foundation, future research should incorporate experimental studies to validate and refine the mathematical predictions. Exploring turbulent flow regimes, three-dimensional geometries, and real biological or industrial conditions will improve the model's realism. Investigation into nanoparticle agglomeration, interaction with biological tissues, and long-term stability is crucial for biomedical usage. Development of controlled heat transfer devices leveraging tunable magnetic and radiative fields, as well as multi-objective optimization of nanoparticle combinations for targeted applications in medical therapy and industrial thermal systems, are promising next steps.

Conflict of interest

The authors declare no competing financial interest.

References

[1] Lone SA, Khan A, Alrabaiah H, Shahab S, Raizah Z, Ali I. Dufour and Soret diffusions phenomena for the chemically reactive MHD viscous fluid flow across a stretching sheet with variable properties. *International Journal of Heat and Fluid Flow*. 2024; 107: 109352. Available from: https://doi.org/10.1016/j.ijheatfluidflow.2024.109352.

[2] Hayat T, Shafiq A, Alsaedi A, Shahzad SA. Unsteady MHD flow over exponentially stretching sheet with slip conditions. *Applied Mathematics and Mechanics*. 2016; 37: 193-208. Available from: https://doi.org/10.1007/s10483-016-2024-8.

[3] Reddy NN, Rao VS, Reddy BR. Chemical reaction impact on MHD natural convection flow through porous medium past an exponentially stretching sheet in presence of heat source/sink and viscous dissipation. *Case Studies in Thermal Engineering*. 2021; 25: 100879. Available from: https://doi.org/10.1016/j.csite.2021.100879.

[4] Neethu TS, Sabu AS, Mathew A, Wakif A, Areekara S. Multiple linear regression on bioconvective MHD hybrid nanofluid flow past an exponential stretching sheet with radiation and dissipation effects. *International Communications in Heat and Mass Transfer*. 2022; 135: 106115. Available from: https://doi.org/10.1016/j.icheatmasstransfer.2022.106115.

[5] Li S, Safdar M, Taj S, Bilal M, Ahmed S, Khan MI, et al. Generalised Lie similarity transformations for the unsteady flow and heat transfer under the influence of internal heating and thermal radiation. *Pramana*. 2023; 97(4): 203. Available from: https://doi.org/10.1007/s12043-023-02672-4.

[6] Mandal IC, Mukhopadhyay S, Vajravelu K. Melting heat transfer of MHD micropolar fluid flow past an exponentially stretching sheet with slip and thermal radiation. *International Journal of Algorithmic Computing and Mathematics*. 2021; 7(2): 31. Available from: https://doi.org/10.1007/s40819-021-00955-1.

[7] Nandhini CA, Jothimani S, Chamkha AJ. Combined effect of radiation absorption and exponential parameter on chemically reactive Casson fluid over an exponentially stretching sheet. *Partial Differential Equations in Applied Mathematics*. 2023; 8: 100534. Available from: https://doi.org/10.1016/j.padiff.2023.100534.

[8] Ragupathi P, Saranya S, Mittal HVR, Al-Mdallal QM. Computational study on three-dimensional convective Casson nanofluid flow past a stretching sheet with Arrhenius activation energy and exponential heat source effects. *Complexity*. 2021; 2021(1): 1-16. Available from: https://doi.org/10.1155/2021/5058751.

[9] Sharma PK, Sharma BK, Mishra NK, Rajesh H. Impact of Arrhenius activation energy on MHD nanofluid flow past a stretching sheet with exponential heat source: A modified Buongiorno's model approach. *International Journal of Modern Physics B*. 2023; 37(32): 2350284. Available from: https://doi.org/10.1142/S0217979223502843.

[10] Ahmad S, Khan MN, Nadeem S. Unsteady three dimensional bioconvective flow of Maxwell nanofluid over an exponentially stretching sheet with variable thermal conductivity and chemical reaction. *International Journal of Ambient Energy*. 2022; 43(1): 6542-6552. Available from: https://doi.org/10.1080/01430750.2022.2029765.

[11] Alqahtani AM, Bilal M, Usman M, Alsenani TR, Ali A, Mahmuod SR. Heat and mass transfer through MHD Darcy Forchheimer Casson hybrid nanofluid flow across an exponential stretching sheet. *ZAMM-Journal of Applied Mathematics and Mechanics*. 2023; 103(6): e202200213.

[12] Mohana CM, Kumar BR. Nanoparticle shape effects on MHD Cu-water nanofluid flow over a stretching sheet with thermal radiation and heat source/sink. *International Journal of Modern Physics B*. 2024; 38(10): 2450151. Available from: https://doi.org/10.1142/S0217979224501510.

[13] Souayeh B, Ramesh K. Numerical scrutinization of ternary nanofluid flow over an exponentially stretching sheet with gyrotactic microorganisms. *Mathematics*. 2023; 11(4): 981. Available from: https://doi.org/10.3390/math11040981.

[14] Khan AA, Khan MN, Ahammad NA, Ashraf M, Guedri K, Galal AM. Flow investigation of second grade micropolar nanofluid with porous medium over an exponentially stretching sheet. *Journal of Applied Biomaterials and Functional Materials*. 2022; 20: 22808000221089782. Available from: https://doi.org/10.1177/22808000221089782.

[15] Gopal D, Jagadha S, Sreehari P, Kishan N, Mahendar D. A numerical study of viscous dissipation with first order chemical reaction and ohmic effects on MHD nanofluid flow through an exponential stretching sheet. *Materials Today: Proceedings*. 2022; 59: 1028-1033. Available from: https://doi.org/10.1016/j.matpr.2022.02.368.

[16] Anwar MI, Firdous H, Zubaidi AA, Abbas N, Nadeem S. Computational analysis of induced magnetohydrodynamic non-Newtonian nanofluid flow over nonlinear stretching sheet. *Progress in Reaction Kinetics and Mechanism*. 2022; 47: 14686783211072712. Available from: https://doi.org/10.1177/14686783211072712.

[17] Li S, Abbas T, Al-Khaled K, Khan SU, Haq EU, Abdullaev SS, et al. Insight into the heat transfer across the dynamics of Burger fluid due to stretching and buoyancy forces when thermal radiation and heat source are significant. *Pramana*. 2023; 97(4): 196. Available from: https://doi.org/10.1007/s12043-023-02678-y.

[18] Hayat T, Asad S, Mustafa M, Alsaedi A. MHD stagnation-point flow of Jeffrey fluid over a convectively heated stretching sheet. *Computers and Fluids*. 2015; 108: 179-185. Available from: https://doi.org/10.1016/j.compfluid.2014.11.016.

[19] Hussain T, Shehzad SA, Hayat T, Alsaedi A, Al-Solamy F, Ramzan M. Radiative hydromagnetic flow of Jeffrey nanofluid by an exponentially stretching sheet. *PLoS ONE*. 2014; 9(8): e103719. Available from: https://doi.org/10.1371/journal.pone.0103719.

[20] Ahmad K, Hanouf Z, Ishak A. Mixed convection Jeffrey fluid flow over an exponentially stretching sheet with magnetohydrodynamic effect. *AIP Advances*. 2016; 6(3): 035024. Available from: https://doi.org/10.1063/1.4945401.

[21] Krishna MV, Kumar AV. Chemical reaction, slip effects and non-linear thermal radiation on unsteady MHD Jeffreys nanofluid flow over a stretching sheet. *Case Studies in Thermal Engineering*. 2024; 55: 104129. Available from: https://doi.org/10.1016/j.csite.2024.104129.

[22] Habib NANN, Arifin NS, Zokri SM, Kasim ARM. Aligned MHD Jeffrey fluid flow containing carbon nanoparticles over exponential stretching sheet with viscous dissipation and Newtonian heating effects. *Journal of Advanced Research in Fluid Mechanics and Thermal Sciences*. 2023; 106(1): 104-115. Available from: https://doi.org/10.37934/arfmts.106.1.104115.

[23] Turkyilmazoglu M. Evidence of stretching/moving sheet-triggered nonlinear similarity flows: Atomization and electrospinning with/without air resistance. *International Journal of Numerical Methods for Heat & Fluid Flow*. 2024; 34(9): 3598-3614. Available from: https://doi.org/10.1108/HFF-04-2024-0254.

[24] Turkyilmazoglu M. Two models on the unsteady heat and fluid flow induced by stretching or shrinking sheets and novel time-dependent solutions. *ASME Journal of Heat and Mass Transfer*. 2024; 146(10): 101802. Available from: https://doi.org/10.1115/1.4065674.

[25] Turkyilmazoglu M, Alotaibi A. Fluid flow between two parallel active plates. *Physica D: Nonlinear Phenomena*. 2024; 470: 134373. Available from: https://doi.org/10.1016/j.physd.2024.134373.

[26] Loretz RA, Loretz TJ. Modified chalcogenide glass equations for the activation energy of crystallization. *Journal of Optics and Photonics Research*. 2024; 1(1): 16-22. Available from: https://doi.org/10.47852/bonviewJOPR42022177.

[27] Ding M, Tang M, Hua Z, Wang X, Zhao Y. Magnetic field sensing by magnetic-fluid-coated capillary long-period fiber gratings. *Journal of Optics and Photonics Research*. 2024; 1(3): 124-130. Available from: https://doi.org/10.47852/bonviewJOPR32021778.

[28] Eslamifar M, Eghbali M. Nonlinear responses and optical limitation of copper nanoparticles by *Z*-scan method. *Journal of Optics and Photonics Research*. 2024; 1(3): 145-150. Available from: https://doi.org/10.47852/bonviewJOPR42021706.

[29] Rehman A, Khan I. Mixed convection flow of hybrid nanofluids with viscous dissipation and dynamic viscosity. *BioNanoScience*. 2024; 14(2): 946-954. Available from: https://doi.org/10.1007/s12668-023-01281-0.

[30] Rehman A, Khun MC, Rezapour S, Inc M, Garalleh HA, Muhammad T. Analytical analysis and heat transfer of CuO and MgO engine oil base nanofluid with the influence of dynamic viscosity, magnetic field, and convective boundary conditions. *ZAMM-Journal of Applied Mathematics and Mechanics*. 2024; 104(6): e202300510.

[31] Rehman A, Salleh Z, Gul T. The impact of the magnetic field and viscous dissipation on the thin film unsteady flow of GO-EG/GO-W nanofluids. *Journal of Physics: Conference Series*. 2019; 1366(1): 012031. Available from: https://doi.org/10.1088/1742-6596/1366/1/012031.

[32] Alshammari S, Ullah Z, Alam MM, Boujelbene M, Ibrahim AO, Abu-Zinadah H. Periodic and time-mean fluctuating heat transfer of Darcy nanofluid along nonlinear radiating plate with heat source/sink and oscillatory amplitude conditions. *Chaos, Solitons & Fractals*. 2025; 194: 116229. Available from: https://doi.org/10.1016/j.chaos.2025.116229.

[33] Majeed S, Ali B, Ullah Z, Shah NA, Hussein AK, Zhu Y. Significance of sinusoidal wall temperature, natural convection, nanoparticle diameter, and nanolayer in water flow subject to a vertical plate via Finite element analysis. *Chaos, Solitons & Fractals*. 2025; 194: 116217. Available from: https://doi.org/10.1016/j.chaos.2025.116217.

[34] Benaissa M, Ullah Z, Dahshan A, Alam MM, Abualnaja KM, Abu-Zinadah H, et al. Heat and mass transfer performance of power-law nanofluid flow with thermal radiation and joule heating aspects: Surface heat flux analysis. *Case Studies in Thermal Engineering*. 2025; 67: 105843. Available from: https://doi.org/10.1016/j.csite.2025.105843.

[35] Alshammari S, Ullah Z, Alam MM, Ibrahim AO, Hamdoun HY, Abu-Zinadah H. Finite difference analysis of turbulent nanofluid and heat fluctuation with oscillatory radiation, gravity and Darcy-Forchheimer porous medium via vertical cone. *Chaos, Solitons & Fractals*. 2025; 193: 116126. Available from: https://doi.org/10.1016/j.chaos.2025.116126.

[36] Khedher NB, Ullah Z, Alam MM, Al Arni S, Elbadawi I, Makinde OD, et al. Significance of thermal conductivity and variable density on heat and mass transfer of MHD second-grade nanofluid along high-temperature polymer surface. *Case Studies in Thermal Engineering*. 2025; 71: 106168. Available from: https://doi.org/10.1016/j.csite.2025.106168.

[37] Noor NAM, Shafie S. Magnetohydrodynamics squeeze flow of sodium alginate-based Jeffrey hybrid nanofluid with heat sink or source. *Case Studies in Thermal Engineering*. 2023; 49: 103303. Available from: https://doi.org/10.1016/j.csite.2023.103303.

[38] Liao SJ. *Homotopy Analysis Method in Nonlinear Differential Equations*. Shanghai: Springer and Higher Education Press; 2012.

[39] Liao S. *Beyond Perturbation: Introduction to the Homotopy Analysis Method*. Boca Raton: Chapman and Hall/CRC; 2003.

[40] Liao S. An optimal homotopy-analysis approach for strongly nonlinear differential equations. *Communications in Nonlinear Science and Numerical Simulation*. 2010; 15(8): 2003-2016. Available from: https://doi.org/10.1016/j.cnsns.2009.09.002.

[41] Liao S. On the homotopy analysis method for nonlinear problems. *Applied Mathematics and Computation*. 2004; 147(2): 499-513. Available from: https://doi.org/10.1016/S0096-3003(02)00790-7.

[42] Rehman A, Khan W, Bonyah E, Abdul Karim SA, Alshehri A, Galal AM. Steady three-dimensional MHD mixed convection couple stress flow of hybrid nanofluid with hall and ion slip effect. *Advances in Civil Engineering*. 2022; 2022(1): 9193875. Available from: https://doi.org/10.1155/2022/9193875.

[43] Rehman A, Jan R, Elamin AEA, Abdel-Khalek S, Inc M. Analytical analysis of steady flow of nanofluid, viscous dissipation with convective boundary condition. *Thermal Science*. 2022; 26(1): 405-410. Available from: https://doi.org/10.2298/TSCI22S1405R.

[44] Rehman A, Saeed A, Salleh Z, Jan R, Kumam P. Analytical investigation of the time-dependent stagnation point flow of a CNT nanofluid over a stretching surface. *Nanomaterials*. 2022; 12(7): 1108. Available from: https://doi.org/10.3390/nano12071108.

[45] Rehman A, Inc M, Salah B, Hussain S. Analytical analysis of silver-water, silver-blood base nanofluid flow over fluctuating disk with the influence of viscous dissipation over fluctuating disk. *Modern Physics Letters B*. 2023; 37(32): 2350113. Available from: https://doi.org/10.1142/S0217984923501130.

[46] Sandeep N, Sulochana C, Rushi Kumar B. Unsteady MHD radiative flow and heat transfer of a dusty nanofluid over an exponentially stretching surface. *Engineering Science and Technology, an International Journal*. 2016; 19(1): 227-240. Available from: https://doi.org/10.1016/j.jestch.2015.06.004.